3

Characterization of charge-coupled devices

Even casual users of CCDs have run across the terms read noise, signal-to-noise ratio, linearity, and many other possibly mysterious sounding bits of CCD jargon. This chapter will discuss the meanings of the terms used to characterize the properties of CCD detectors. Techniques and methods by which the reader can determine some of these properties on their own and why certain CCDs are better or worse for a particular application are discussed in the following chapters. Within the discussions, mention will be made of older types of CCDs. While these are generally not available or used anymore, there is a certain historical perspective to such a presentation and it will likely provide some amusement for the reader along the way.

One item to keep in mind throughout this chapter and in the rest of the book is that all electrons look alike. When a specific amount of charge is collected within a pixel during an integration, one can no longer know the exact source of each electron (e.g., was it due to a stellar photon or is it an electron generated by thermal motions within the CCD itself ?). We have to be clever to separate the signal from the noise. There are two notable quotes to cogitate on while reading this text. The first is from an early review article on CCDs by Craig Mackay (1986), who states: “The only uniform CCD is a dead CCD.” The second is from numerous discussions I have had with CCD users and it is: “To understand your signal, you must first understand your noise.”

3.1 Quantum efficiency

The composition of a CCD is essentially pure silicon. This element is thus ultimately responsible for the response of the detector to various wavelengths of light. The wavelength dependence of silicon can be understood in an instant by glancing at Figure 3.1. Shown here is the length of silicon needed

https://doi.org/10.1017/CBO9780511807909.005

for a photon of a specific wavelength to be absorbed. Absorption length is defined as the distance for which 63% (1/*e*) of the incoming photons will be absorbed. Figure 3.1 clearly shows that, for light outside the range of about 3500 to over 8000 Å, the photons (1) pass right through the silicon, (2) get absorbed within the thin surface layers or gate structures, or (3) simply reflect off the CCD surface. At short wavelengths, 70% or more of the photons are reflected, and for very short wavelengths (as for long wavelengths) the CCD becomes completely transparent. Thus the quantum efficiency of a typical CCD device will approximately mirror the photon absorption curve for silicon. Shortward of ~2500 Å (for thinned devices) or about 25 Å (for thick devices) the detection probability for photons increases again. However, owing to their much higher energy, these photons lead to the production of

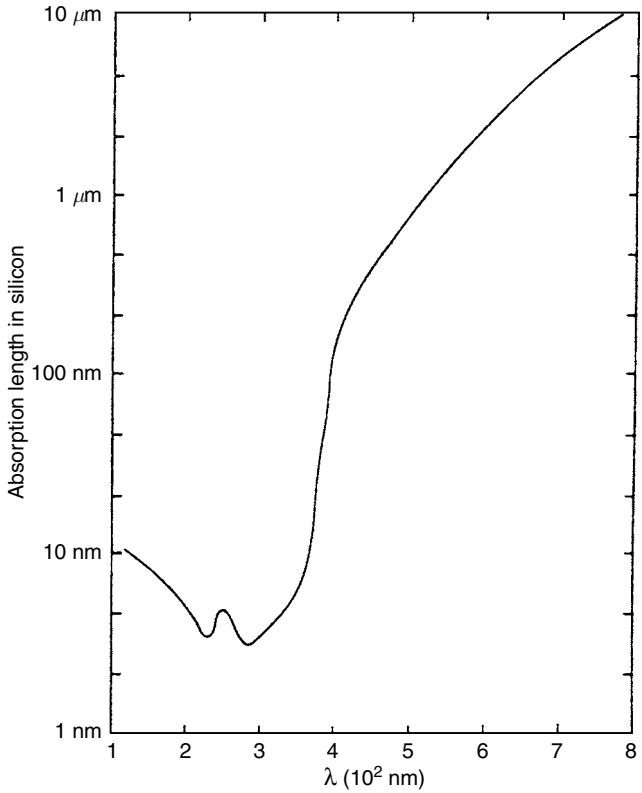

Fig. 3.1. The photon absorption length in silicon is shown as a function of wavelength in nanometers. From Reicke (1994).

multiple electron–hole pairs within the silicon and may also produce damage to the CCD itself (see Chapter 7).

CCD quantum efficiencies are therefore very dependent on the thickness of the silicon that intercepts the incoming photons. This relation between absorption probability and CCD thickness is why front-side illuminated (thick) devices are more red sensitive (the photons have a higher chance of absorption) and why they have lower overall (blue) QEs (since the gate structures can be close to or even exceed the necessary absorption depths of as small as only a few atomic layers). A few front-side CCDs have been produced with special gate structures that are transparent to incoming blue and UV photons. In thinned devices, the longest wavelength photons are likely to pass right through the CCD without being absorbed at all.

Figure 3.2 shows the quantum efficiencies for various imaging devices. Note that the y scale is logarithmic and the much superior QE provided by CCDs over previous detectors. Figure 3.3 shows a selection of modern CCD QEs. The large difference in QE that used to exist between thinned and thick CCDs is now mostly eliminated due to manufacturing processes

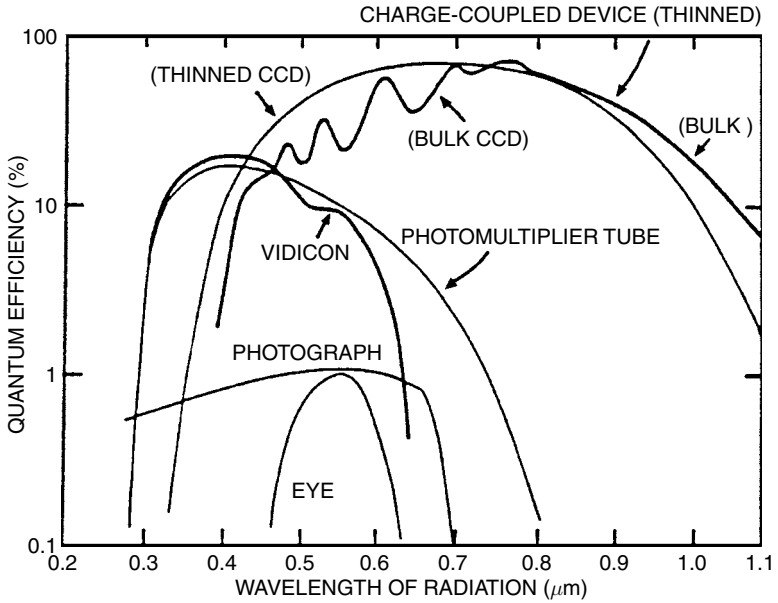

Fig. 3.2. QE curves for various devices, indicating why CCDs are a quantum leap above all previous imaging devices. The failure of CCDs at optical wavelengths shorter than about 3500 Å has been essentially eliminated via thinning or coating of the devices (see Figure 3.3).

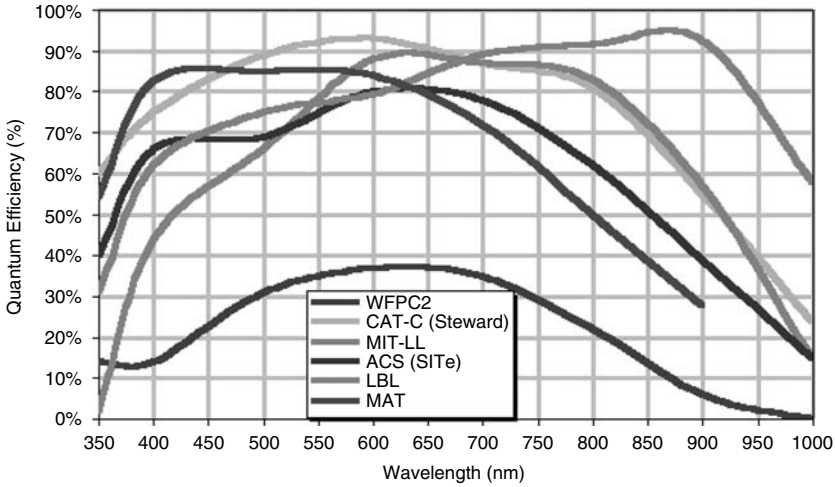

Fig. 3.3. QE curves for a variety of CCDs. WFPC2 is the second generation wide-field/planetary camera aboard HST, CAT-C is a new generation SITe CCD used in a mosaic imager at the University of Arizona's 90" telescope on Kitt Peak, MIT-LL is a CCD produced at the MIT Lincoln Laboratories and optimized for red observations, ACS is the Hubble Space Telescope Advanced Camera for Surveys SITe CCD, LBL is a Lawrence Berkeley Lab high resistivity, "deep depletion" CCD with high red QE, and MAT is a front-side, processed CCD showing high blue QE.

and coatings although other differences (such as location of peak QE, cosmic ray detection, etc.) remain. Quantum efficiency or QE curves allow one quickly to evaluate the relative collecting power of the device as a function of wavelength. Measured QE curves, such as in Figure 3.3 and those shown in the literature, are generally assumed to be representative of each and every pixel on the device, that is, all pixels of a given device are assumed to work identically and have the same wavelength response. This is almost true, but it is the "almost" that makes flat fielding of a CCD necessary. In addition, the QE curves shown or delivered with a particular device may only be representative of a "typical" device of the same kind, but they may not be 100% correct for the exact device of interest.

The quantum efficiency of a CCD is temperature sensitive especially in the red wavelength region. It has long been known that measurement of the QE at room temperature is a poor approximation to that which it will have when operated cold. Thus QE curves should be measured at or near the operating temperature at which the CCD will be used. As an example of the temperature sensitivity of the efficiency of a CCD, Figure 3.4 shows

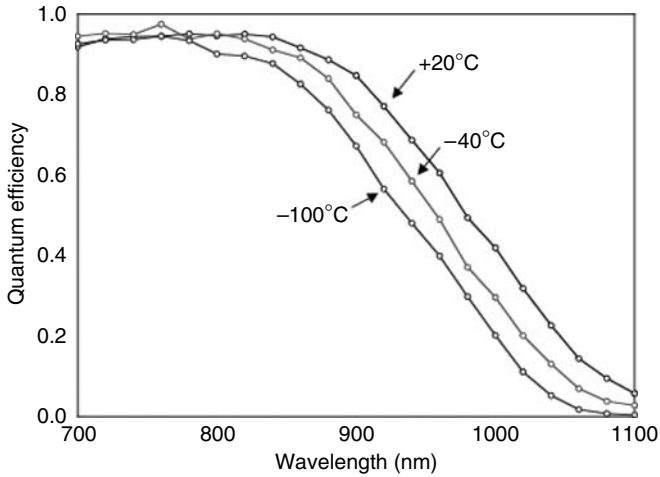

Fig. 3.4. Sensitivity of the quantum efficiency of a MIT/LL CCD for three operating temperatures. The blue sensitivity is little affected by a change in operating temperature but the red QE can change by a factor of two. The use of such devices requires a balance of higher operating temperature and keeping the dark current under control.

three QE measurements of the same CCD for temperatures of +20° C (∼room temperature), −40°C, and −100°C (∼operating temperature). Note that the variations are small at 8000 Å but increase to 20% at 9000–10 000 Å. The curves in this plot would lead one to the conclusion that operating a CCD at room temperature is the best thing to do. However, Section 3.5 will show us why this is not the case and a compromise between operating temperature (i.e., dark current) and delivered QE must be used.

A recent advance in the manufacture of CCDs is to use high resistivity silicon. Typical CCDs you have used have a resistivity of 20–200 ohm-cm or maybe up to 300 ohm-cm and are made on 10–40 micron epi.[1] The above resistivity and thickness values for Si wafers are fairly standard today and lend themselves to easy etching for thinning (10–20 micron final thickness). Starting with bulk silicon and a new process called the float-zone technique, resistivities up to 5000–10 000 ohm-cm are possible. Adding in a bias voltage to the optically transparent back-side substrate and using a thick layer of 45 to 350 micron epi, each pixel in a high resistivity CCD can be fully depleted resulting in very high red QE and deep pixel wells. Figure 3.5 shows the relationship between Si resistivity, depletion depth, and the bias voltage used.

[1] epi (pronounced "ep'-pea") is CCD lingo for epitaxial silicon, which is the Si wafer type used to make CCDs. An example was shown in Figure 2.8.

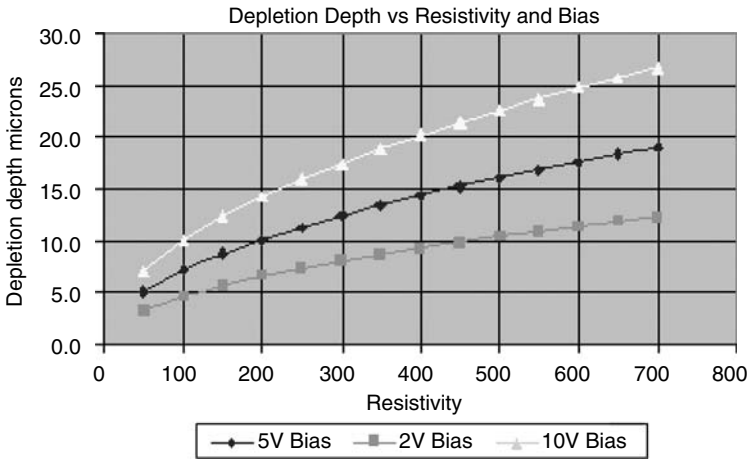

Fig. 3.5. Laboratory measurements of the depletion depth in a pixel vs. the CCD silicon resistivity for three different bias voltages. We see that one can deplete deeper (larger) pixels with higher resistivity silicon assuming the use of a larger bias voltage.

These "deep depletion" CCDs collect up to about 300 000 photoelectrons deep in a pixel where they are more likely to stay given the high resistivity. Higher resistivity silicon wafers require very special care in their production and much higher purity tolerances of the Si wafers, thus are more costly to produce. The internal Si lattice structures must be highly uniform and the level of unwanted impurities in the Si must be very near zero. Until the past few years, production of such Si was not possible and today the Lawrence Berkeley Lab (LBL) and MIT/Lincoln Labs are the leaders in making such devices. Figure 3.3 shows the superior red QE of a LBL high resistivity CCD. As we noted in our discussion of Figure 3.1, the thickness of a CCD is important in the QE it attains, and thus deep depletion devices have large well depths to aid in the improvement of their red QE. The resistivity of the Si and the deep pixels both come into play when one considers charge diffusion within a CCD. We will discuss charge diffusion in some detail below.

Placing an antireflection (AR) coating on a CCD (both for visible and near-UV light) increases the QE and extends the range of good QE well into the 3000 Å region. The need for AR coatings comes from the fact that silicon, like most metallic substances, is a good reflector of visible light. If you ever have a chance to hold a CCD, you will easily see just how well the surface does indeed reflect visible light. All the QE curves in Figure 3.3 have the overall shape expected based on the absorption properties of silicon as shown

in Figure 3.1. Graphical illustrations of QE curves almost always include photon losses due to the gate structures, electron recombination within the bulk silicon itself, surface reflection, and, for very long or short wavelengths, losses due to the almost complete lack of absorption by the CCD. Given that all these losses are folded together into the QE value for each wavelength, it should be obvious that changes within the CCD structure itself (such as radiation damage or operating temperature changes) can cause noticeable changes in its quantum efficiency.

Measurement of the quantum efficiency of a CCD is usually performed with the aid of complicated laboratory equipment including well-calibrated photodiodes. Light at each wavelength is used to illuminate both the CCD and the photodiode, and the relative difference in the two readings is recorded. The final result of such an experiment is an absolute QE curve for the CCD (with respect to the calibrated diode) over the range of all measured wavelengths.

To measure a CCD QE curve yourself, a few possibilities exist. You may have access to a setup such as that described above. Measurements can also be made at the telescope itself. One good method of QE measurement for a CCD consists of employing a set of narrow-band filters and a few spectrophotometric standard stars. Performing such a task will provide a good relative QE curve and, if one knows the filter and telescope throughput well, a good absolute QE curve. A detailed reference as to what is involved in the measurement of a spectrophotometric standard star is provided by Tüg *et al.* (1977). When producing a QE curve by using the above idea, the narrow-band filters provide wavelength selection while the standard stars provide a calibrated light source. A less ambitious QE curve can be produced using typical broad-band (i.e., Johnson) filters, but the final result is not as good because of the large bandpasses and throughput overlap of some of the filters. In between a detailed laboratory setup and the somewhat sparse technique of using filters at the telescope, another method exists. Using an optics bench, a calibrated light source covering the wavelength range of interest, and some good laboratory skills, one can produce a very good QE curve for a CCD and can even turn the exercise into a challenging classroom project.

3.2 Charge diffusion

Once an electron is captured in a CCD pixel, the voltages applied during integration attempt to hold it in place. However, situations arise within a CCD pixel that provide a finite possibility for any given electron to wander out of

https://doi.org/10.1017/CBO9780511807909.005

its collection pixel and into a neighboring pixel. This process is called charge diffusion and until recently it was noted but of low significance compared with other noise and readout issues. Today CCDs are of excellent quality and have very low readout noise, good pixel registration on the array, and reside in high quality optical systems. These facts mean that CCD imaging now has the ability to show great detail of any optical aberrations and geometric distortions. Even items such as better mechanical tolerances in instrumentation can reveal noticeable focus variations as materials breathe with thermal changes. Given CCDs with deep pixel wells, large format front-side illuminated thinned devices, and the related improvements to modern astronomical instrumentation, the effects of charge diffusion on the point-spread function are noticeable.

A few ways in which charge diffusion can occur may be useful to discuss. Imagine a deep (geometrically long) pixel modeled after that which is shown in Figure 2.4 (also refer to Figure 3.5). Electrons produced by long wavelength photons are captured in the front-side illuminated pixel near the bottom, far from the applied voltages in the front gates. Thus the potential well for these electrons is more like a potential dip. Given the right circumstances, an electron can move into a neighboring pixel. Another example would be impurities in the silicon material the CCD was manufactured from. These variations in the Si lattice can slightly bend or slightly redirect the potential within a pixel and provide weak spots from which electron escape is possible. Ways to mitigate electron loss are the use of higher potential voltages (although this can lead to other issues such as logic glow or shorting on the array), higher resistivity Si (as discussed above) to more tightly hold the electrons (the Si lattice) in place, or to use small pixels (but these have lower red QE and small well depths). Again, we see that compromise and specific application come into play and can be tuned into the CCD as a part of its production process.

Charge diffusion often varies significantly across a CCD, especially thinned devices as they are not equal thickness everywhere. For example, the Hubble Space Telescope ACS wide field camera thinned CCD shows a variation in the core of the PSF, caused by charge diffusion, across the field of view. The variation is 30–40% at 5000 Å with larger variations at shorter wavelengths (Krist, 2004, HST ACS user manual). The effects of charge diffusion are not to be taken lightly. The ACS/WFC suffers a loss of about 0.5 magnitudes in its limiting magnitude at short wavelengths and near 0.2 magnitudes elsewhere. Charge diffusion is especially important in thinned devices that undersample the point-spread function.

3.3 Charge transfer efficiency

As we mentioned in the previous chapter, charge transfer efficiency or CTE is a measure of the fraction of the charge that is successfully transferred for each pixel transfer. CTE values of 0.999 995 or more are typical in good modern CCDs. For a CCD with 1024×1024 pixels, the charge collected in the last pixel readout has shifted 2048 times thus the CTE must be nearly 100% in order to preserve the charge in each pixel during readout. CTI (charge transfer inefficiency) is 1–CTE or numerically near 10^{-5} or 10^{-6} in value. CTI can be and usually is different in the vertical and horizontal directions. The loss in charge from a CCD pixel containing N electrons that is shifted 1024 times vertically and 1024 times horizontally is given by $L(e) = N(1024 * \mathrm{CTI}(H) + 1024 * \mathrm{CTI}(V))$ or, if a single CTI value is given, $L(e) = 2048 * N * \mathrm{CTI}$. CCDs with poor CTE generally show charge tails in the direction opposite readout for bright stars. These tails are the charge left behind as the image is shifted out.

The standard method for measuring CTE is to use X-ray stimulation of a CCD with a Fe^{55} source. CCDs are good X-ray detectors (see Chapter 7) and for a specific X-ray source such as Fe^{55}, each X-ray photon collected produces ~ 1620 electrons.[1] A CCD is exposed to X-ray illumination and the resulting image readout. An X-ray transfer plot is made of signal in DN (y-axis) vs. running pixel number on the x-axis. Often hundreds of rows are summed together to increase the signal generated by the weak X-ray source. If the CCD has good CTE, a horizontal line will be seen at 1620 electrons (assuming a gain of 1.0). If the CTE is poor, this line starts at 1620 electrons (for rows close to the output amplifier) but tilts toward lower signal values for pixels further away from the output amplifier. This behavior indicates a loss of charge being transferred due to poor CTE. The CTE of a given CCD will generally degrade rapidly with decreasing operating temperature and is also a function of the clocking pulse shape and speed.

X-ray transfer techniques become imprecise for CTEs that are $> 0.999\,99$ and for CCDs with very large formats. For these CCDs, more sensitive CTE measurement techniques are required. A detailed discussion of the many intricacies of CTE in CCDs, how it is measured, and additional CTE measurement techniques are presented in Janesick (2001).

[1] Remember that for optical photon detection, one photon collected produces one photoelectron, regardless of its wavelength. For the much higher energy X-rays, a single photon collected produces multiple electrons in proportion to the photon's energy.

3.4 Readout noise

CCDs can be though of as having three noise regimes: read noise, shot noise, and fixed pattern noise. In astronomy, we speak of these as read noise limited, photon noise limited, and flat field uncertainties. A plot of the log of the standard deviation of the signal (y-axis) vs. the log of the signal itself (x-axis) for a CCD is called the photon transfer curve. Read noise (or any noise independent of signal level) sets a noise floor for a device. Upon illumination, photon or Poisson noise raises the sigma measured following a $N^{1/2}$ slope (see Chapter 4). Finally, for large signal values, pixel to pixel variations due to processing errors and photomask mis-alignment begin to dominate. This latter noise is proportional to the signal and rises with a slope of 1.0. Full well sets in at some very high illumination and the slope of the photon transfer curve turns over or breaks. We discuss read noise below and the total noise and flat fielding in the next chapter.

Readout noise, or just read noise, is usually quoted for a CCD in terms of the number of electrons introduced per pixel into your final signal upon readout of the device. Read noise consists of two inseparable components. First is the conversion from an analog signal to a digital number, which is not perfectly repeatable. Each on-chip amplifier and A/D circuit will produce a statistical distribution of possible answers centered on a mean value.[1] Thus, even for the hypothetical case of reading out the same pixel twice, each time with identical charge, a slightly different answer may be produced. Second, the electronics themselves will introduce spurious electrons into the entire process, yielding unwanted random fluctuations in the output. These two effects combine to produce an additive uncertainty in the final output value for each pixel. The average (one sigma) level of this uncertainty is the read noise and is limited by the electronic properties of the on-chip output amplifier and the output electronics (Djorgovski, 1984).[2]

The physical size of the on-chip amplifier, the integrated circuit construction, the temperature of the amplifier, and the sensitivity (generally near 1–4 μV/detected photon, i.e., collected photoelectron) all contribute to the read noise for a CCD. In this micro world, the values for electronic noise are highly related to the thermal properties of the amplifier, which in turn determines the sensitivity to each small output voltage. Amazing as it seems, the readout speed, and thus the rate at which currents flow through the on-chip

[1] The distribution of these values is not necessarily Gaussian (Merline & Howell, 1995).

[2] We note here that the level of the read noise measured, or in fact any noise source within a CCD, can never be smaller than the level of discretization produced by the A/D converter (see Sections 2.4 and 3.8).

amplifier, can cause thermal swings in the amplifier temperature, which can affect the resulting read noise level.[1] Generally, slower readout speeds produce lower read noise but this reduced readout speed must be weighed against the overall camera duty cycle. Small effects caused by amplifier heating can even occur between the readout of the beginning and end of a single CCD row, as the last charge packets pass through a slightly hotter circuit. Increasing the physical size of the already small microamplifiers can alleviate these small temperature swings, but larger amplifiers have a higher input capacitance, thereby lowering the sensitivity of the amplifier to small voltages.

Additional work on amplifier design, methods of clocking out pixels, and various semiconductor doping schemes can be used to increase the performance of the output electronics. Production techniques for integrated circuits have also contributed greatly to improved noise performance. An example of this improvement is the highly precise registration of each layer of a pixel's material and structure during production leading to more uniform electronic fields within the device and thus less resistive noise. CCD manufacturers invest large efforts into balancing these issues to produce very low read noise devices. Many details of the various aspects of read noise in CCDs are discussed by Janesick and Elliott (1992).

In the output CCD image, read noise is added into every pixel every time the array is readout. This means that a CCD with a read noise of 20 electrons will, on average, contain 20 extra electrons of charge in each pixel upon readout. High read noise CCDs are thus not very good to use if co-addition of two or more images is necessary. The final resultant image will not be quite as good as one long integration of the same total time, as each co-added image will add in one times the read noise to every pixel in the sum. However, for modern CCDs (see Section 4.4), read noise values are very low and are hardly ever the dominant noise with which one must be concerned. Good read noise values in today's CCDs are in the range of 10 electrons per pixel per read or less. These values are far below read noise levels of ten years ago, which were as high as 50–100 electrons, and even those are well down from values of 300–500 or more electrons/pixel/read present in the first astronomical CCDs.

In Section 4.3, we will discuss a simple method by which one may determine for oneself the read noise of a given CCD. This determination can be performed with any working CCD system and does not require special equipment, removal of the CCD from the camera dewar, or even removal from the telescope.

[1] Figure 6.8a, spectrum a, shows this effect for the first few columns in each row.

3.5 Dark current

Every material at a temperature much above absolute zero will be subject to thermal noise within. For silicon in a CCD, this means that when the thermal agitation is high enough, electrons will be freed from the valence band and become collected within the potential well of a pixel. When the device is readout, these dark current electrons become part of the signal, indistinguishable from astronomical photons. Thermal generation of electrons in silicon is a strong function of the temperature of the CCD, which is why astronomical use generally demands some form of cooling (McLean, 1997b). Figure 3.6 shows a typical CCD dark current curve, which relates the amount of thermal dark current to the CCD operating temperature. Within the figure the theoretical relation for the rate of thermal electron production is given.

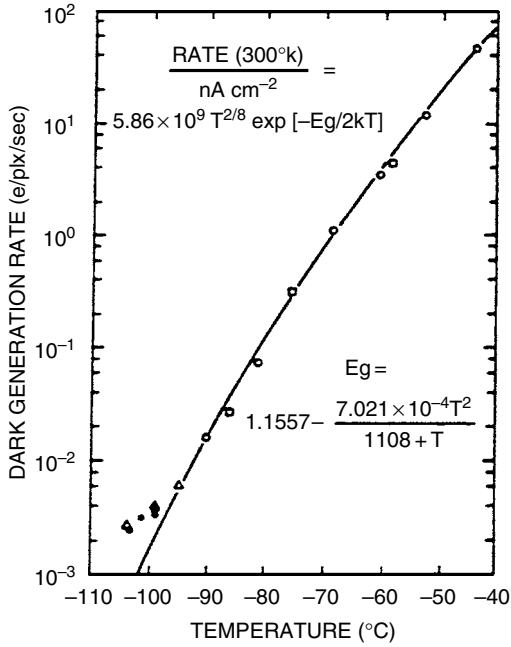

Fig. 3.6. Experimental (symbols) and theoretical (line) results for the dark current generated in a typical three-phase CCD. The rate of dark current, in electrons generated within each pixel every second, is shown as a function of the CCD operating temperature. E_g is the band gap energy for silicon. From Robinson (1988a).

Dark current for a CCD is usually specified as the number of thermal electrons generated per second per pixel or as the actual current generated per area of the device (i.e., picoamps cm^{-2}). At room temperature, the dark current of a typical CCD is near 2.5×10^4 electrons/pixel/second. Typical values for properly cooled devices range from 2 electrons per second per pixel down to very low levels of approximately 0.04 electrons per second for each pixel. Although 2 electrons of thermal noise generated within a pixel every second sounds very low, a typical 15 minute exposure of a faint astronomical source would include 1800 additional (thermal) electrons within each CCD pixel upon readout. These additional charges cannot, of course, be uniquely separated from the photons of interest after readout. The dark current produced in a CCD provides an inherent limitation on the noise floor of a CCD. Because dark noise has a Poisson distribution, the noise actually introduced by thermal electrons into the signal is proportional to the square root of the dark current (see Section 4.4).

Cooling of CCDs is generally accomplished by one of two methods. The first, and usually the one used for scientific CCDs at major observatories, is via the use of liquid nitrogen (or in some cases liquid air). The CCD and associated electronics (the ones on or very near the actual CCD itself, called the head electronics) are encased in a metal dewar under vacuum. Figure 3.7 shows a typical astronomical CCD dewar (Brar, 1984; Florentin-Nielsen, Anderson, & Nielsen, 1995). The liquid nitrogen (LN2) is placed in the dewar and, although not in direct physical contact with the CCD, cools the device to temperatures of near $-100°$ C. Since LN2 itself is much colder than this, CCDs are generally kept at a constant temperature ($\pm 0.1°$ C) with an on-board heater. In fact, the consistency of the CCD temperature is very important as the dark current is a strong function of temperature (Figure 3.6) and will vary considerably owing to even modest changes in the CCD temperature.

A less expensive and much less complicated cooling technique makes use of thermoelectric cooling methods. These methods are employed in essentially all "off-the-shelf" CCD systems and allow operation at temperatures of -20 to $-50°$ C or so, simply by plugging the cooler into an electrical outlet. Peltier coolers are the best known form of thermoelectric cooling devices and are discussed in Martinez & Klotz (1998). CCD operation and scientific quality imaging at temperatures near $-30°$ C is possible, even at low light levels, due to advances in CCD design and manufacturing techniques and the use of multipinned phase operation (see Chapter 2). Other methods of cooling CCDs that do not involve LN2 are discussed in McLean (1997a).

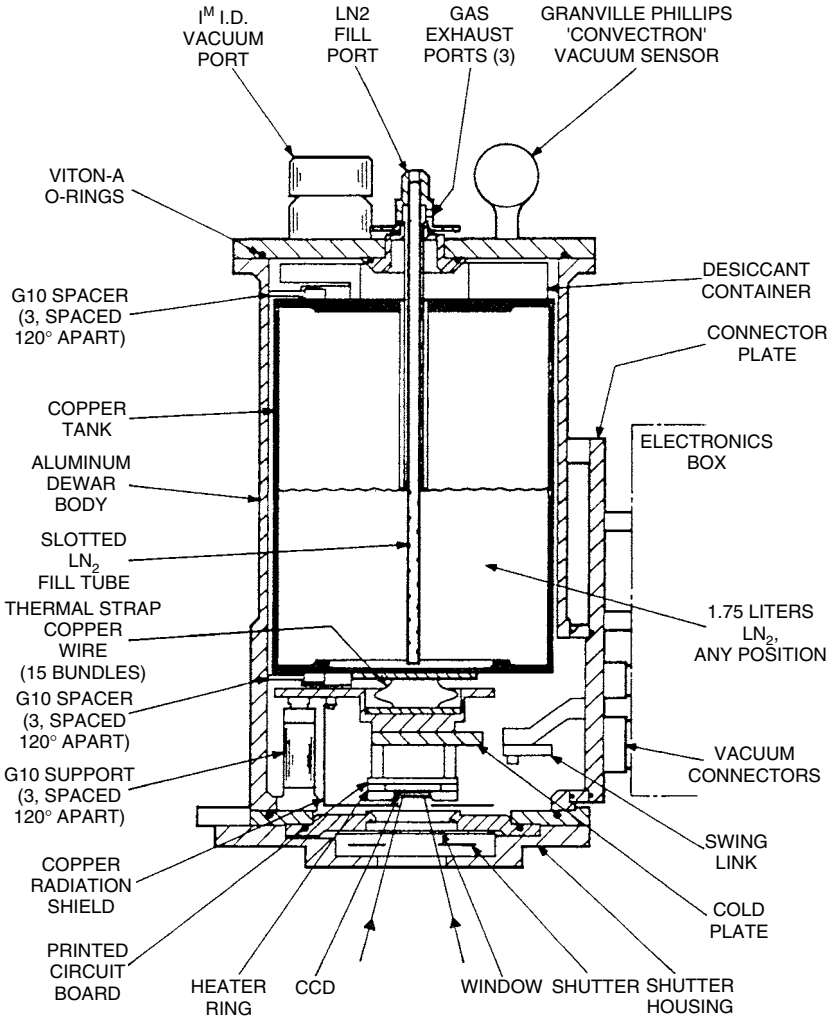

Fig. 3.7. A typical CCD dewar. This is the Mark-II Universal dewar originally produced in 1984 at Kitt Peak National Observatory. The dewar held 1.75 liters of liquid nitrogen providing a CCD operating time of approximately 12 hours between fillings. This dewar could be used in up-looking, down-looking, and side-looking orientations. From Brar (1984).

The amount of dark current a CCD produces depends primarily on its operating temperature, but there is a secondary dependence upon the bulk properties of the silicon used in the manufacture. Even CCDs produced on the same silicon wafer can have slightly different dark current properties.

Today's CCDs are made from high purity epi wafers produced with low occurrences of integrated circuit error. These factors have greatly reduced many of the sources of dark current even at warmer temperatures. As with most of the noise properties of a given CCD, custom tailoring the CCD electronics (such as the bias level and the readout rate) can produce much better or much worse overall dark current and noise performance.

3.6 CCD pixel size, pixel binning, full well capacity, and windowing

This section is a combination of a few related topics concerning the amount of charge that can be stored within a given pixel during an integration. We have seen that CCD thinning, MPP operation, and small physical pixel size all place limitations on the total number of electrons that can be collected within a pixel. The general rule of thumb is that the physically larger the pixel (both in area and in thickness) the more charge that it can collect and store.

The amount of charge a pixel can hold in routine operation is termed its full well capacity. A Kodak CCD with 9-micron pixels (meaning 9 microns on a side for the projected area, but giving no indication of the thickness of the CCD) operating in MPP mode has a full well capacity per pixel of 85 000 electrons. In contrast, a SITe CCD with 24-micron pixels can have a full well capacity per pixel of over 350 000 electrons. CCDs have been produced today which have 1 million electron well depths per pixel. While this value is highly desirable, it is not without compromise. Keep in mind our above discussion of charge diffusion.

When we discussed the method by which a CCD is readout (Chapter 2) it was stated that each row is shifted in turn into the output register and then digitized, and the resulting DN value is sent off to the computer. During this process, each pixel's value is increased on average by one times the read noise. If we could add up the charge within say 4 pixels before they are digitized, we would get a final signal level equal to $\sim$4 times each single pixel's value, but only one times the read noise. This process is called on-chip binning and, if selected, occurs prior to readout within the CCD output register (Smith, 1990b; Merline & Howell, 1995). Pixels can be binned (summed) in both vertical and horizontal directions. "On-chip" means that the accumulated charge from each pixel involved in the binning is brought together and summed before the process of A/D conversion occurs. This summing process is done in the output register and is limited by the size of the "pixels" within this register. Generally, the output register pixels can

https://doi.org/10.1017/CBO9780511807909.005

hold five to ten times the charge of a single active pixel. This deeper full well capacity of the output register pixels allows pixel summing to take place.

Older CCD systems that allowed on-chip binning had plug boards mounted on the sides of the dewar. Certain combinations of the plug wires produced different on-chip binning patterns and users could change these to suit their needs. Today, most CCDs have the ability to perform pixel summing as a software option (Leach, 1995). Binning terminology states that normal operation (or "high resolution" as it is called by many low-cost CCDs) is a readout of the CCD in which each pixel is read, digitized, and stored. This is called 1×1 binning or unbinned operation. Binning of 2×2 would mean that an area of four adjacent pixels will be binned or summed on-chip within the output register during readout, but before A/D conversion. The result of this binning operation will produce only one "superpixel" value, which is digitized and stored in the final image; the original values in each of the four summed pixels are lost forever. Mainly for spectroscopic operation, binning of 3×1 is commonly used, with the 3 being in the direction perpendicular to the dispersion. Binning of CCD pixels decreases the image resolution, usually increases the final signal-to-noise value of a measurement, and reduces the total readout time and final image size. For example, a 1024×1024 CCD binned 2×2 will have a final image size of only 512×512 pixels and the readout time will be reduced by about a factor of four.

Pixel binning gives flexibility to the user for such applications as (using a high binning factor) quick readout for focus tests, nights with poor seeing, or very low surface brightness observations. Spectroscopic observations with a CCD, high spatial resolution imaging, or bright object observations will benefit from the use of a low binning factor. Binning factors that are very large (say 40×40 pixels) might be of use in some rare cases, but they will be limited by the total amount of charge one can accumulate in a single superpixel of the output register.

A related function available with some CCDs is "windowing." Windowing allows the user to choose a specific rectangular region (or many regions) within the active area of the CCD to be readout upon completion of the integration. The CCD window is often specified by providing the operating software with a starting row and column number and the total number of x, y pixels to use. For example, using a 2048×2048 CCD to make high-speed imaging observations would be difficult, but windowing the CCD to use only the first 512 rows and columns (0, 0, 512, 512) allows for much faster readout and requires far less storage for the image data. The use of subregion readout for astronomical CCDs is often the heart of fast imaging cameras such as UltraCam and OPTIC. New generation OTCCDs allow for fast readout via

https://doi.org/10.1017/CBO9780511807909.005

the use of not only fast readout electronics (available to all modern CCDs) but by having no single CCD larger than about 512×512 pixels.

Of course, the object of interest must be positioned within these first 512 rows and columns, and not at the center of the CCD as may be usual. Other applications of CCD windowing would include choosing a cosmetically good subregion of a large CCD or only a rectangular strip to readout from a larger square CCD, when making spectroscopic observations. CCD windowing is independent of any on-chip binning, and one can both window and bin a CCD for even more specific observational needs.

3.7 Overscan and bias

In an attempt to provide an estimate of the value produced by an empty or unexposed pixel within a CCD, calibration measurements of the bias level can be used.[1] Bias or zero images allow one to measure the zero noise level of a CCD. For an unexposed pixel, the value for zero collected photoelectrons will translate, upon readout and A/D conversion, into a mean value with a small distribution about zero.[2] To avoid negative numbers in the output image,[3] CCD electronics are set up to provide a positive offset value for each accumulated image. This offset value, the mean "zero" level, is called the bias level. A typical bias level might be a value of 400 ADU (per pixel), which, for a gain of $10\,e^-/ADU$, equals 4000 electrons. This value might seem like a large amount to use, but historically temporal drifts in CCD electronics due to age, temperature, or poor stability in the electronics, as well as much higher read noise values, necessitated such levels.

[1] For more on bias frames and their use in the process of CCD image calibration, see Chapter 4.

[2] Before bias frames, and in fact before any CCD frame is taken, a CCD should undergo a process known as "wiping the array." This process makes a fast read of the detector, without A/D conversion or data storage, in order to remove any residual dark current or photoelectron collection that may have occurred during idle times between obtaining frames of interest.

[3] Representation of negative numbers requires a sign bit to be used. This bit, number 15 in a 16-bit number, is 0 or 1 depending on whether the numeric value is positive or negative. For CCD data, sacrificing this bit for the sign of the number leaves one less bit for data, thus reducing the overall dynamic range. Therefore, most good CCD systems do not make use of a sign bit. One can see the effects of having a sign bit by viewing CCD image data of high numeric value but displayed as a signed integer image. For example, a bright star will be represented as various grey levels, but at the very center (i.e., the brightest pixels) the pixel values may exceed a number that can be represented by 14 bits (plus a sign). Once bit 15 is needed, the signed integer representation will be taken by the display as a negative value and the offending pixels will be displayed as black. This is due to the fact that the very brightest pixel values have made use of the highest bit (the sign bit) and the computer now believes the number is negative and assigns it a black (negative) greyscale value. This type of condition is discussed further in Appendix.

https://doi.org/10.1017/CBO9780511807909.005

To evaluate the bias or zero noise level and its associated uncertainty, specific calibration processes are used. The two most common ones are: (1) overscan regions produced with every object frame and (2) usage of bias frames. Bias frames amount to taking observations without exposure to light (shutter closed), for a total integration time of 0.000 seconds. This type of image is simply a readout of the unexposed CCD pixels through the on-chip electronics, through the A/D converter, and then out to the computer producing a two-dimensional bias or zero image.

Overscan strips, as they are called, are a number of rows or columns (usually 32) or both that are added to and stored with each image frame. These overscan regions are not physical rows or columns on the CCD device itself but additional pseudo-pixels generated by sending additional clock cycles to the CCD output electronics. Both bias frames and overscan regions are techniques that allow one to measure the bias offset level and, more importantly, the uncertainty of this level.

Use of overscan regions to provide a calibration of the zero level generally consists of determining the mean value within the overscan pixels and then subtracting this single number from each pixel within the CCD object image. This process removes the bias level pedestal or zero level from the object image and produces a bias-corrected image. Bias frames provide more information than overscan regions, as they represent any two-dimensional structure that may exist in the CCD bias level. Two-dimensional (2-D) patterns are not uncommon for the bias structure of a CCD, but these are usually of low level and stable with time. Upon examination of a bias frame, the user may decide that the 2-D structure is nonexistent or of very low importance and may therefore elect to perform a simple subtraction of the mean bias level value from every object frame pixel. Another possibility is to remove the complete 2-D bias pattern from the object frame using a pixel-by-pixel subtraction (i.e., subtract the bias image from each object image). When using bias frames for calibration, it is usually best to work with an average or median frame composed of many (10 or more) individual bias images (Gilliland, 1992). This averaging eliminates cosmic rays,[1] read noise variations, and random fluctuations, which will be a part of any single bias frame.

Variations in the mean zero level of a CCD are known to occur over time and are usually slow drifts over many months or longer, not noticeable changes from night to night or image to image. These latter types of changes

[1] Cosmic rays are not always cosmic! They can be caused by weakly radioactive materials used in the construction of CCD dewars (Florentin-Nielsen, Anderson, & Nielsen, 1995).

indicate severe problems with the readout electronics and require correction before the CCD image data can be properly used.

Producing a histogram of a typical averaged bias frame will reveal a Gaussian distribution with the mean level of this distribution being the bias level offset for the CCD. We show an example of such a bias frame histogram in Figure 3.8. The width of the distribution shown in Figure 3.8 is related to the read noise of the CCD (caused by shot noise variations in the CCD electronics (Mortara & Fowler, 1981)) and the device gain by the following expression:

$$\sigma_{\mathrm{ADU}} = \frac{\text{Read noise}}{\text{Gain}}.$$

Note that σ is used here to represent the width (FWHM) of the distribution not the usual definition for a Gaussian shape. For example, in Figure 3.8, $\sigma = 2$ ADU.

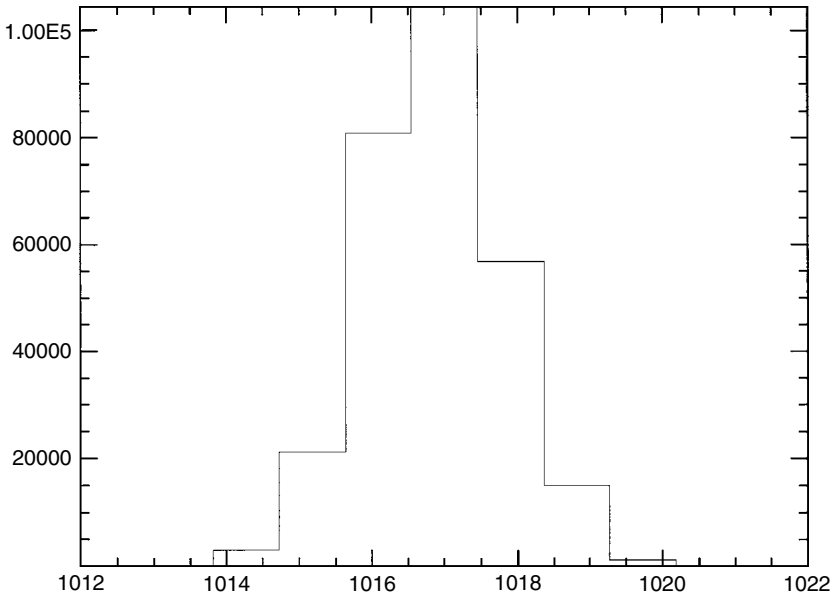

Fig. 3.8. Histogram of a typical bias frame showing the number of pixels vs. each pixel ADU value. The mean bias level offset or pedestal level in this Loral CCD is near 1017 ADU, and the distribution is very Gaussian in nature with a FWHM value of near 2 ADU. This CCD has a read noise of 10 electrons and a gain of 4.7 e^-/ADU.

https://doi.org/10.1017/CBO9780511807909.005

3.8 CCD gain and dynamic range

The gain of a CCD is set by the output electronics and determines how the amount of charge collected in each pixel will be assigned to a digital number in the output image. Gain values are usually given in terms of the number of electrons needed to produce one ADU step within the A/D converter. Listed as electrons/Analog-to-Digital Unit (e^-/ADU), common gain values range from 1 (photon counting) to 150 or more. One of the major advantages of a CCD is that it is linear in its response over a large range of data values. Linearity means that there is a simple linear relation between the input value (charge collected within each pixel) and the output value (digital number stored in the output image).

The largest output number that a CCD can produce is set by the number of bits in the A/D converter. For example, if you have a 14-bit A/D, numbers in the range from zero to 16 383 can be represented.[1] A 16-bit A/D would be able to handle numbers as large as 65 535 ADU.

Figure 3.9 provides a typical example of a linearity curve for a CCD. In this example, we have assumed a 15-bit A/D converter capable of producing output DN values in the range of 0 to 32 767 ADU, a device gain of 4.5 e^-/ADU, and a pixel full well capacity of 150 000 electrons. The linearity curve shown in Figure 3.9 is typical for a CCD, revealing that over most of the range the CCD is indeed linear in its response to incoming photons. Note that the CCD response has the typical small bias offset (i.e., the output value being nonzero even when zero incident photons occur), and the CCD becomes nonlinear at high input values. For this particular CCD, nonlinearity sets in near an input level of 1.17×10^5 photons (26 000 ADU), a number still well within the range of possible output values from the A/D.

As we have mentioned a few times already in this book, modern CCDs and their associated electronics provide high-quality, low-noise output. Early CCD systems had read noise values of 100 times or more of those today and even five years ago, a read noise of 15 electrons was respectable. For these systems, deviations from linearity that were smaller than the read noise were rarely noticed, measurable, or of concern. However, improvements that have lowered the CCD read noise provide an open door to allow other subtleties to creep in. One of these is device nonlinearities. Two types of nonlinearity are quantified and listed for today's A/D converters. These are integral nonlinearity and differential nonlinearity. Figure 3.10 illustrates these two types of A/D nonlinearity.

[1] The total range of values that a specific number of bits can represent equals $2^{(\text{number of bits})}$, e.g., $2^{14} = 16\,384$. CCD output values are zero based, that is, they range from 0 to $2^{(\text{number of bits})} - 1$.

https://doi.org/10.1017/CBO9780511807909.005

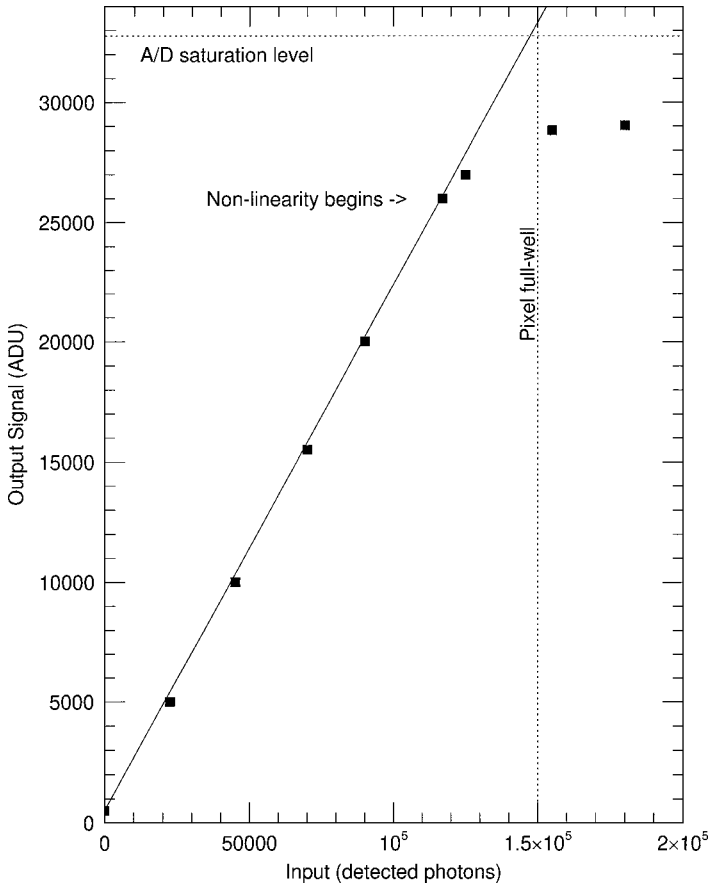

Fig. 3.9. CCD linearity curve for a typical three-phase CCD. We see that the device is linear over the output range from 500 ADU (the offset bias level of the CCD) to 26 000 ADU. The pixel full well capacity is 150 000 electrons and the A/D converter saturation is at 32 767 ADU. In this example, the CCD nonlinearity is the limiting factor of the largest usable output ADU value. The slope of the linearity curve is equal to the gain of the device.

A/D converters provide stepwise or discrete conversation from the input analog signal to the output digital number. The linearity curve for a CCD is determined at various locations and then drawn as a smooth line approximation of this discrete process. Differential nonlinearity (DNL) is the maximum deviation between the line approximation of the discrete process and the A/D step used in the conversion. DNL is often listed as ±0.5 ADU meaning that for a given step from say 20 to 21 ADU, fractional counts of 20.1,

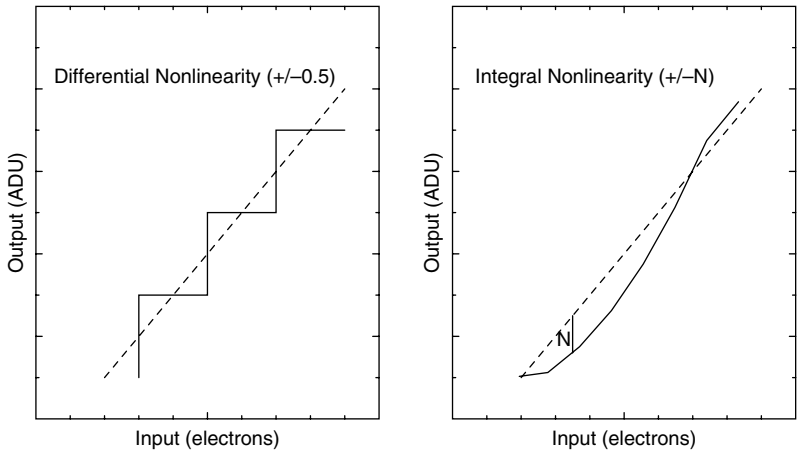

Fig. 3.10. The two types of CCD nonlinearity are shown here in cartoon form. Differential nonlinearity (left) comes about due to the finite steps in the A/D conversion process. Here we see that the linearity curve (dashed line) cuts through each step at the halfway point yielding a DNL of ±0.5 ADU. Integral nonlinearity (right) is more complex and the true linearity curve (solid line) may have a simple or complex shape compared with the measured curve (dashed line). A maximum deviation (N) is given as the INL value for an A/D and may occur anywhere along the curve and be of either sign. Both plots have exaggerated the deviation from linearity for illustration purposes.

20.2, etc. up to 20.499 99 will yield an output value of 20 while those of 20.5, 20.6, etc. will yield an output value of 21. Astronomers call this type of nonlinearity digitization noise and we discuss it in more detail below. Integral nonlinearity (INL) is of more concern as it is the maximum departure an A/D will produce (at a given convert speed) from the expected linear relationship. A poor quality A/D might have an INL value of 16 LSB (least significant bits). The value of 16 LSB means that this particular A/D has a maximum departure from linearity of 4 bits ($2^4 = 16$) throughout its full dynamic range. If the A/D is a 16-bit device and all 16 bits are used, bits 0–3 will contain any INL at each ADU step. If one uses the top 12 bits, then bits 4–7 are affected.

How the INL comes into play for an observer is as follows. For a gain of say 5 electrons/ADU, an INL value of 16 can cause a nonlinear deviation of up to 80 electrons in the conversion process at its maximum deviation step (see Figure 3.10). Thus, at the specific A/D step that has the maximum deviation, an uncertainty of ±80 electrons will occur but be unknown to the user. This is a very unacceptable result for astronomy, but fine for digital

cameras or photocopiers that usually have even higher values of INL caused by their very fast readout (conversion) speeds.

A good A/D will have an INL value near 2–2.5 LSB or, for the above example, a maximum deviation of only 10 electrons. While this sounds bad, a 16-bit A/D can represent 65 535 values making the 10 electrons only a 0.02% nonlinearity. However, a 12-bit A/D, under similar circumstances, would have a 0.2% nonlinearity. The lesson here is to use a large dynamic range (as many bits as possible) to keep the nonlinearity as small as possible. We can now obtain A/D converters with low values for INL and which have 18 bits of resolution. So for a given modern CCD, nonlinearity is usually a small but nonzero effect.

Three factors can limit the largest usable output pixel value in a CCD image: the two types of saturation that can occur (A/D saturation and exceeding a pixel's full well capacity; see Sections 2.2.4 and 2.4) and nonlinearity. For the CCD in the example shown in Figure 3.9, A/D saturation would occur at an output value of $32\,767 \cdot 4.5 = 147\,451$ input photons. The pixel full well capacity is 150 000 electrons; thus pixel saturation will occur at a value of 33 333 ADU (150 000/4.5). Both full well and A/D saturations would produce noticeable effects in the output data such as bleeding or flat-topped stars. This particular example, however, illustrates the most dangerous type of situation that can occur in a CCD image. The nonlinear region, which starts at 26 000 ADU, is entered into before either type of saturation can occur. Thus, the user could have a number of nonlinear pixels (for example the peaks of bright stars) and be completely unaware of it. No warning bells will go off and no flags will be set in the output image to alert the user to this problem. The output image will be happy to contain (and the display will be happy to show) these nonlinear pixel values and the user, if unaware, may try to use such values in the scientific analysis.

Thus it is very important to know the linear range of your CCD and to be aware of the fact that some pixel values, even though they are not saturated, may indeed be within the nonlinear range and therefore unusable. Luckily, most professional grade CCDs reach one of the two types of saturation before they enter their nonlinear regime. Be aware, however, that this is almost never the case with low quality, inexpensive CCD systems that tend to use A/Ds with fewer bits, poor quality electronics, or low grade (impure) silicon. Most observatories have linearity curves available for each of their CCDs and some manufacturers include them with your purchase.[1] If uncertain of the linear range of a CCD, it is best to measure it yourself.

[1] A caution here is that the supplied linearity curve may only be representative of your CCD.

One method of obtaining a linearity curve for a CCD is to observe a field of stars covering a range of brightness. Obtain exposures of say 1, 2, 4, 8, 16, etc. seconds, starting with the shortest exposure needed to provide good signal-to-noise ratios (see Section 4.4) for most of the stars and ending when one or more of the stars begins to saturate. Since you have obtained a sequence that doubles the exposure time for each frame, you should also double the number of incident photons collected per star in each observation. Plots of the output ADU values for each star versus the exposure time will provide you with a linearity curve for your CCD.

A common, although not always good, method of determining the value to use for the CCD gain, is to relate the full well capacity of the pixels within the array to the largest number that can be represented by your CCD A/D converter. As an example, we will use typical values for a Loral 512×1024 CCD in current operation at the Royal Greenwich Observatory. This CCD has 15-micron pixels and is operated as a back-side illuminated device with a full well capacity of 90 000 electrons per pixel. Using a 16-bit A/D converter (output values from 0 to 65 535) we could choose the gain as follows. Take the total number of electrons a pixel can hold and divide it by the total ADU values that can be represented: $90\,000/65\,536 = 1.37$. Therefore, a gain choice of $1.4\,e^-$/ADU would allow the entire dynamic range of the detector to be represented by the entire range of output ADU values. This example results in a very reasonable gain setting, thereby allowing the CCD to produce images that will provide good quality output results.

As an example of where this type of strategy would need to be carefully thought out, consider a CCD system designed for a spacecraft mission in which the A/D converter only had 8 bits. A TI CCD was to be used, which had a full well capacity of 100 000 electrons per pixel. To allow imagery to make use of the total dynamic range available to the CCD, a gain value of 350 ($\sim 100\,000/2^8$) e^-/ADU was used. This gain value certainly made use of the entire dynamic range of the CCD, allowing images of scenes with both shadow and bright light to be recorded without saturation. However, as we noted before, each gain step is discrete, thereby making each output ADU value uncertain by $\pm$ the number of electrons within each A/D step. A gain of $350\,e^-$/ADU means that each output pixel value has an associated uncertainty of upto ~ 1 ADU, which is equal to, in this case, upto 350 electrons, a large error if precise measurements of the incident flux are desired. The uncertainty in the final output value of a pixel, which is caused by the discrete steps in the A/D output, is called digitization noise and is discussed in Merline & Howell (1995).

To understand digitization noise let us take, as an example, a CCD that can be operated at two different gain settings. If we imagine the two gain values to be either 5 or 200 e^-/ADU and that a particular pixel collects 26 703 electrons (photons) from a source, we will obtain output values of 5340 and 133 ADU respectively. Remember, A/D converters output only integer values and so any remainder is lost. In this example, 3 and 103 electrons respectively are lost as the result of the digitization noise of the A/D. More worrisome than this small loss of incident light is the fact that while each ADU step in the gain equals 5 e^-/ADU case can only be incorrect by < 5 electrons, the gain equals 200 e^-/ADU case will be uncertain by upto 200 electrons in each output ADU value. Two hundred electrons/pixel may not seem like much but think about trying to obtain a precise flux measurement for a galaxy that covers thousands of pixels on a CCD image or even a star that may cover tens of pixels. With an error of 200 electrons/pixel multiplied by tens or many more pixels, the value of a galaxy's surface brightness at some location or similarly a stellar magnitude would be highly uncertain.

The gain of a particular CCD system is set by the electronics and is generally not changeable by the user or there may be but a few choices available as software options. How A/D converters actually determine the assignment of the number to output for each pixel and whether the error in this choice is equally distributed within each ADU step is a detailed matter of interest but lies outside the scope of this book. A discussion of how the digitization noise affects the final output results from a CCD measurement is given in Merline & Howell (1995) and a detailed study of ADCs used for CCDs is given in Opal (1988).

Major observatories provide detailed information to a potential user (generally via internal reports or web pages) as to which CCDs are available. Table 3.1 gives an example of some of the CCDs in use in various instruments at the European Southern Observatory (ESO) in Chile. When planning an observational program, one must not only decide on the telescope and instrument to use, but must also be aware of the CCD(s) available with that instrument. The properties of the detector can be the most important factor in determining the success or failure of an observational project. Thus, some care must be taken in deciding which CCD, with its associated properties, you should use to accomplish your science objectives.

In our above discussion of the gain of a CCD, we mentioned the term dynamic range a few times but did not offer a definition. The dynamic range of any device is the total range over which it operates or for which it is sensitive. For audio speakers this number is usually quoted in decibels, and

https://doi.org/10.1017/CBO9780511807909.005

Table 3.1. *Some CCDs available at the European Southern Observatory (ESO)*

Instrument	Telescope	Type	CCD	Size (pixels)	Pixel Size (microns)	Pixel Scale (arcsec)	Readout Time (seconds)	Gain (e^-/ADU)	Read Noise electrons	Notes
EMMI	3.6-m NTT	Spectrograph Red channel	MIT/LL	2048×4096	15	0.17	18–48	1.4	4	Thinned, back-side
EMMI	3.6-m NTT	Spectrograph Blue channel	MIT/LL	1024×1024	24	0.37	40	1.4, 2.8	7	Thinned, back-side
FORS2	8-m VLT	Imager/ Spectrograph	MIT/LL	2048×4096	15	0.12	40	1.1	6	Deep Depletion, Red optimized
OmegaCam	2.6-m VST	Wide-Field imager	E2V	2048×4096	15	0.21	45	3	5	

this tradition has been used for CCDs as well. Keeping to the idea of decibels as a measure of the dynamic range of a CCD, we have the expression

$$D(\text{dB}) = 20 \times \log_{10}(\text{full well capacity/read noise}).$$

Thus a CCD with a full well capacity of 100 000 electrons per pixel and a read noise of 10 electrons would have a dynamic range of 80 dB. A more modern (and more useful) definition for the dynamic range of a CCD is simply the ratio of the (average) full well capacity of a pixel to the read noise of the device, namely

$$D = (\text{full well capacity/read noise}).$$

In the example above, $D = 10\,000$.

3.9 Summary

This chapter has concentrated on defining the terminology used when discussing CCDs. The brief nature of this book does not allow the many more subtle effects, such as deferred charge, cosmic rays, or pixel traps, to be discussed further nor does it permit any discussion of the finer points of each of the above items. The reader seeking a deeper understanding of the details of CCD terminology (a.k.a., someone with a lot of time on his or her hands) is referred to the references given in this chapter and the detailed reading list in Appendix A. Above all, the reader is encouraged to find some CCD images and a workstation capable of image processing and image manipulation and to spend a few hours of time exploring the details of CCDs for themselves.

As a closing thought for this chapter, Table 3.2 provides a sample of the main properties of two early astronomical CCDs and a few modern devices. The sample shown tries to present the reader with an indication of the typical properties exhibited by CCDs. Included are those of different dimension, of different pixel size, having front and back illumination, cooled by LN2 or thermoelectrically, and those available from different manufacturers. Information such as that shown in Table 3.2 can be found at observatory websites and in greater detail at CCD manufacturers' websites. Most have readily available data sheets for the entire line of CCDs they produce. Each example for a given CCD in Table 3.2 is presented to show the range of possible properties and does not imply that all CCDs made by a given company are of the listed properties. Most manufacturers produce a wide variety of device types. Appendix B provides a listing of useful CCD websites.

Table 3.2. *Typical Properties of Two Old and Six Modern Example CCDs*

	RCA	TI	Kodak	E2V	SITe	Sarnoff	STA (WIYN)	MIT/LL
Pixel Format	320 × 512	800 × 800	2048 × 2048	2048 × 4608	2048 × 2048	600 × 2400	3840 × 3952 OT	2048 × 4096
Pixel Size (microns)	30	15	9	13	12	13	12	15
Detector Size (mm)	10 × 15	12 × 12	18 × 18	27 × 62	25 × 25	6 × 25	50	31 × 62
Pixel Full Well (e^-)	350 000	50 000	100000	150000	110000	> 20000	> 70000	> 200000
Illumination	Front	Back	Front	Back	Back	Back	Back	Back
Peak QE (%) / Wavelength (A)	70/4500	70/6500	45/6500	90/5000	85/6500	99/6600	96/5500	95/7700
Read Noise (e^-)	80	15	15	3	6	6	< 5	2.5
CTE	0.99995	0.999985	0.99998	0.999995	0.99999	0.99999	0.999998	0.999995
Operating Temp (C)	−100	−120	−30	−85	−85	−60	−60	−110
Typical Gain used (e^-/ADU)	13.5	5	5	1.5	3	5	1.5	1.37

3.10 Exercises

1. Using only the data presented in Figures 3.1 and 3.2, draw a quantum efficiency curve expected for a typical CCD. Why might real QE curves be different?
2. Discuss two major reasons why CCDs are better detectors than the human eye. Are there instances in which the eye is a better detector? What "type" of A/D converter does the eye have?
3. Design a detailed observing plan or laboratory experiment that would allow you to measure the quantum efficiency of a CCD. Discuss the specific light sources (astronomical or laboratory) you might use and over what band-passes you can work. How accurate a result would you expect?
4. Why is charge diffusion important to consider in a deep depletion CCD? Using the standard physics equation for diffusion, can you estimate the area over which electrons from one pixel will spread in a CCD as a function of time? (You will have to look up the properties of bulk silicon and keep in mind the operating temperatures and voltages.)
5. Make a list of the various CCD properties that contribute to CTI. For each, discuss a method for mitigation.
6. When does read noise get introduced into each pixel of a CCD during the readout process? How could you design a CCD to have zero read noise?
7. A CCD has a typical background level of 100 ADUs per pixel and a read noise of 6 electrons rms. An image is obtained that contains only read noise. What range of values would one expect to find in any pixel on the array? How would these values be distributed around the 100 ADU value?
8. Using the data presented in Figure 3.6, estimate the dark current for that CCD at room temperature. Given your answer, how do video or digital cameras record scenes that are not saturated by thermal noise?
9. Estimate the dark current for the CCD illustrated in Figure 3.6 at liquid nitrogen temperatures, at –120 °C, at dry ice temperatures, and if using a thermoelectric cooler. What level of dark current is acceptable?
10. Do the numbers discussed in Section 3.6 concerning pixel size and full well capacity agree with your calculations from Question 8 in Chapter 2?
11. Discuss an observational application that might require CCD windowing and one that might require CCD binning. What limits the practical use of CCD binning on any given chip?

https://doi.org/10.1017/CBO9780511807909.005

12. Detail the difference between overscan and bias. How are each related to a "zero" or bias image?
13. Why do CCDs have a bias level at all?
14. What is so important about a device being linear in its response to light?
15. For a CCD with a full well capacity of 90 000 electrons per pixel and a 12-bit A/D, what gain value would you choose and why? How might your choice change if the CCD became nonlinear at 65 000 electrons?
16. Design a detailed observing plan or laboratory experiment that would allow you to measure the linearity of a CCD. Discuss the specific light sources (astronomical or laboratory) you might use and the sequence of integrations you would take. What measurements would you make from the collected images? Over what band-passes would you work and how accurate a result would you expect?
17. Which type of nonlinearity is more acceptable in a CCD for spectroscopic observations? For photometric observations? What would the output from an A/D converter look like if the DNL was 0.1 instead of 0.5? What if the INL was 32?
18. What is "digitization noise" and under what conditions is it undesirable?
19. Using Table 3.2, discuss the best CCD to use for spectroscopic observations of sources with faint continua but very bright emission lines. What is the best CCD to use if you were attempting to measure very weak stellar absorption lines?
20. Compare the dynamic range of a CCD to that of a typical sub-woofer speaker. Compare it to a police-car siren.

https://doi.org/10.1017/CBO9780511807909.005